Journal Homepage: http://ijcpe.uobaghdad.edu.iq
Iraqi Journal of Chemical and Petroleum Engineering
Vol. 26 No. 1 (March 2025) 77 – 88
EISSN: 2618-0707, PISSN: 1997-4884

Investigation of the effects of chitosan-zinc nanoparticles Ch-ZnO NPs on phenotypic biofilm formation of Acinetobacter baumannii and cytotoxicity assay

Yousif Salih Abdul Jabbar [a], Umut Gazi [a], Mais Emad Ahmed [b, *]

a Department of Medical Microbiology and Clinical Microbiology, Faculty of Medicine, Near East University, Nicosia 99138, Cyprus
b Department of Biology, College of Science, University of Baghdad, Baghdad, Iraq

Abstract

The research aimed to create chitosan zinc oxide nanoparticles (Ch-ZnO NPs) for use as agents to combat biofilms produced by Acinetobacter baumannii. The Ch-ZnO NPs were produced using chitosan biomass as a cost-effective, eco-friendly material for synthesis purposes. The properties of the produced nanoparticles were analyzed through a range of methods. Fourier transform infrared spectroscopy (FTIR) carried out chemical structure identification and analysis. The maximum absorption peak, at 235 nm was confirmed through UV spectrophotometry. The X-ray diffraction (XRD) varied the hexagonal crystal structure with a particle size measurement of 34 nm. Surface morphology was probed using atomic force microscopy (AFM) and field emission scanning electron microscopy (FESEM). Further details on the particle structure were obtained through high-resolution transmission electron microscopy (HR-TEM). To assess how Ch-ZnO NPs perform in real-world scenarios when dealing with Acinetobacter baumannii bacterial infections and tackling biofilms effectively was the focus of the study, with exploration into its impact on cytotoxicity using the cell line model of A375 for potential medical applications. The research findings indicated that Ch-ZnO NPs exhibited capabilities in inhibiting biofilm growth from drug-resistant Acinetobacter baumannii bacteria strains with an IC50 concentration of 2.0 g/mL. The assessment of cell mortality rates highlighted a rise, in cell death among the treated cells from the application of Ch-ZnO NPs. The research revealed that Ch-ZnO NPs demonstrated ant-biofilm properties and cytotoxic effects, which suggest their potential for use is significant. This study emphasizes the promise of Ch-ZnO NPs as an efficient option for treating infections resistant to multiple antibiotics.

Keywords: Acinetobacter baumannii; Biofilm, Chitosan; Nanocomposites; Zinc oxide.

Received on 06/11/2024, Received in Revised Form on 13/12/2024, Accepted on 13/12/2024, Published on 30/03/2025

https://doi.org/10.31699/IJCPE.2025.1.8

1- Introduction

As Acinetobacter baumannii (A. baumannii) contains specific features that allow it to attack the immune system of the body, it is a major source of nosocomial infections. A. baumannii can grow on both biotic and abiotic surfaces and readily takes up antibiotic resistance determinants. This victory against antibiotics has been made possible by a variety of mechanisms of resistance or determinants, both transmissible and non-transmissible [1]. One of the ways Acinetobacter baumannii is harmful is, by creating biofilms which are essential in causing ventilator-associated pneumonia (VAP). Biofilm formation allows the bacteria to stick to surfaces easily and avoid antibiotics and immune system attacks, from the host leading to lasting infections [2].

Biological biofilms of bacteria are organized communities of a few species that are enclosed in a protective polysaccharide matrix made of proteins, lipids, and extracellular DNA, Complicated communications among the biofilm community allow infections to become resistant to multiple obstacles, medicines, and host defenses [3].

In addition to bacterial virulence factors, food acquisition, interactions among communities, and genetic modulation of virulence the phenotype A. baumannii is the cause of several diseases. The quorum-sensing community interactions between cells nearby are vital to the A. baumannii population's viability [4]. Scientists are doing a job of creating ways to fight against bacteria that produce biofilms and show resistance to multiple drugs [5]. Green synthesis of metal oxide nanoparticles has gained significant attention for its sustainable approach and wide applications in biotechnology and healthcare [6]. Often utilized as an organic synthesis route, plant extracts ZnO nanoparticles are a potent antibacterial agent against a variety of bacterial species due to their diverse shapes and sizes and limited surface area, which allow them to capture microbial cells [7]. One of the most important nanoparticles of metal oxide is zinc oxide (ZnO NPs), a naturally occurring material with an array of biological applications (anti-inflammatory, anti-bacterial).

*Corresponding Author: Email: mais.emad@sc.uobaghdad.edu.iq

Multiple investigations have demonstrated that the quorum sensing system could be a target for drugs against bacteria that prevent the creation of biofilms over time [8].

For certain reasons, chitosan appears to be an appropriate choice among organic polymers. First off, although it has functional groups where metal ions can be attached, it is believed to be an intriguing option for creating Nano-hybrids, in addition, chitosan (CS) is a polysaccharide that's non-toxic, biocompatible, and biodegradable [9].

With the developments of nanotechnology, Chitosan can now be generated with a variety of morphologies and ways to prepare [10]. Because of its greater aspect ratio relative to other morphologies, the nano-fibrillar (NF) form can show notable features in applications in medicine [10]. Using the MTT, plaque, and Real-time PCR methods, nanoparticles made of zinc oxide (ZnO NPs) and chitosan-ZnO nanostructures (Ch-ZnO NPs) have been generated to assess their cytotoxicity and inhibitory effect against microorganism expansion in vitro [11]. The focus of this study was to measure the anti-biofilm activity of environmentally conscious, synthesized chitosan-zinc oxide nanoparticles (Ch-ZnO NPs) on the growth of biofilms. By Acinetobacter baumannii. Based on the distinctive characteristics of chitosan, which were mentioned above, this research suggests that Ch-ZnO NPs added to chitosan-based biocomposites show improved effects, against Gram bacteria that are resistant to multiple drugs while also showing promise for safe use, in various applications because of their unique structural and functional characteristics.

2- Experimental work

2.1. Material and methods

Sample collections: A total of 100 clinical samples were collected from wound swabs collected from patients at the resident hospital in AL Yarmouk Teaching Hospital. The samples were cultured immediately after collection for diagnostic purposes. Additionally, were identified primarily by culturing on MacConkey at 37C for 24 h. and confirmed by the VITEC 2 system [12]. Conforming to the guidelines published by the Clinical & Laboratory Standards Institute: CLSI Guidelines 2023, susceptibility testing takes place on Mueller Hinton agar plates via the disk method [13].

a. Synthesis of ZnO NPs

ZnO NPs were produced using an easy co-precipitation method [14]. First, a room-temperature 0.5 mL solution of zinc acetate dehydrate was made. The zinc acetate dehydrate solution (pH adjusted to 7) was subsequently combined with 0.5 mL of sodium hydroxide solution to generate a light, milky suspension of ZnO NPs. Finally, the previously mentioned suspension was repeatedly rinsed with deionized water under a magmatic starrier to get rid of excess zinc acetate and other pollutants.

b. Preparation of Ch-ZnO NPs

Ch-ZnO nanoparticles (Ch-ZnO NPs) were synthesized using the co-precipitation method at room temperature. The process began with the preparation of chitosan (CS) solution by dissolving 2 g of powdered chitosan in 100% acetic acid. This mixture was stirred on a magnetic stirrer for 2 hours to achieve a uniform suspension. Next, 0.5 mL of sodium hydroxide solution was added to the chitosan suspension and stirred for an additional 10 minutes. The resulting mixture was then used to deposit coatings, forming a light milky suspension, which was designated as Ch-ZnO NPs. To purify the suspension, it was washed multiple times with deionized water and ethanol to remove excess zinc acetate and other impurities. Finally, the purified suspension was dried using a microwave at 120°C for 15 minutes [15].

c. Characterization of Ch-ZnO NPs

Understanding the distinctive features of nanoparticles requires characterization. The shapes and sizes of the nanoparticles were identified using the following techniques: Field Emission Scanning Electron Microscopy (FE-SEM) was employed to graphically represent and evaluate the surface morphology, particle size distribution, shape of the particle or crystal, agglomeration of nanoparticles, surface functionalization, and single-particle evaluations. UV-visible (UV-DRS) is used to investigate the optical properties of the materials, while atomic force microscopy (AFM) is used to determine the diameter and height of NPs in 3D vision. (XRD) is a method used in materials science to identify a material's crystallographic structure. Functional groups of prepared nanostructures in the range of 4000–400 nm were examined by Fourier-transform infrared spectroscopy (FT-IR, RX I, PerkinElmer, Inc., USA) at a resolution of 4 cm1 and Zeta Potential (ZP) and energy dispersive X-ray (EDX) [16].

d. MIC determination

Using Eppendorf tubes and the technique of microdilution of broth, the minimal concentration of Ch-ZnO NPs that limits bacterial growth was identified (MIC). The microbial inoculum was generated in MHB and its concentration was reduced to 100 UFC/µl. Six tubes were utilized to create two-fold serial dilutions of Ch-ZnO NPs (1000, 500, 250, 125, and 64 µg/µl) using MHB. The tubes were followed by incubation at 37° C for a full day. Results were then obtained by identifying signs of growth of bacteria in every tube, during which the sub-MIC could be determined [17].

e. Estimation of biofilm formation

Bacteria grown in broth were utilized to produce the 1:100 diluted biofilm inoculums, which were

subsequently transferred to the 200 l well. The broth is used in the negative control wells (200 l of BHI supplemented with 1% glucose per well). Every strain completed three different tests [18]. Under static conditions, the inoculated plate was covered with a lid and incubated aerobically for 24–30 hours at 35–37 °C. Numerous bacteria MDR Multidrug resistance, using a micro titer-plate reader (GloMax/ Promega-USA), the optical density (OD) of each well was measured at 630 nm. Three standard deviations (SD) above the median OD of the negative control, or ODc, is the cut-off value for the adverse control. Average OD for the negative control plus (3× SD of the negative control) yields ODc.

f. Effect of Ch-ZnO NPs on biofilm formation

In this experiment, we utilized 96 well microtiter plates, for testing purposes. The strains under examination were grown in CPI at a temperature of 37°C for 24 hours. In each well of the plate, a volume of 100, µl bacterial inoculum was added after dilution to a 0.5 McFarland standard. A sub-inhibitory amount of Ch-ZnO NPs was then added to each well with a volume of 100 µl followed by incubation at 37°C for 48 hours. A positive control was maintained using culture without the Nano formulation. For the negative control, a clear broth was employed. After the incubation period elapsed in each well of the microplate setup and the contents were removed for processing; the microplates were subsequently subjected to drying at a temperature of 60°C for 45 minutes. Thoroughly rinsed multiple times using sterile saline solution to ensure cleanliness and sterility maintenance. Following this cleaning step; a volume of 200 milliliters was exposed to staining with a solution containing 0. l percent crystal violet. Allowed to sit at ambient room temperature for 15 minutes before undergoing three rounds of washing with sterile saline solution. Subsequently; the optical density (OD) measurement of each well was conducted at a wavelength of 630 nanometers to evaluate characteristics or properties associated with the samples analyzed in the microplates.

g. Cytotoxicity assay of Ch-ZnO NPs

The MTT test was employed to evaluate the cell viability for various doses of Ch-ZnO NPs (1, 1.5, 2, 2.5, and 3µg/ml) against malignant cells (A375 cells) and typical fibroblast cells (WRL68 cells) were redistributed at required concentration into culture vessels, flasks or plates whatever needed and incubated at 37°C in 5% CO2 incubator. Cell concentration was achieved by counting the cells using the haemocytometer and applying the formula.

Total Cell Count/ml: cell count x dilution factor (sample volume) x 10^4 [20].

Protocol:

- Tumor cells ($1x10^4$ – $1x10^6$ cells/mL) were grown in 96 flat well micro-titer plates, in a final volume of 200mL complete culture medium RPMI-1640 per each well. The microplate was covered by sterilized parafilm and shacked gently.
- The plates were incubated at 37°C, 5% CO_2 for 24hrs.
- After incubation, the medium was removed and two-fold serial dilutions of the desired compound (12.5, 25, 50, 100, 200, 400 mg/mL) were added to the wells.
- Triplicates were used per each concentration as well as the controls (cells treated with serum free medium). Plates were incubated at 37°C, 5% CO_2 for selected exposure time (24 hours).
- After exposure, 10 ml of the MTT solution was added to each well. Plates were further incubated at 37°C, 5% CO_2 for 4 hours.

The media were carefully removed and 100mL of solubilization solution was added per each well for 5 min. The absorbance was determined by using an ELISA reader at a wavelength of 575 nm. The data of optical density was subjected to statistical analysis in order to calculate the viability rate.

3- Results and discussion

3.1. Isolation and identification

A total of sixty-four Isolates were confirmed as A. baumannii, displayed pale and round colonies on MacConkey agar, and were non-lactose fermenters as shown in Fig. 1, the conformation was carried out by the VITEK 2 system considered a reliable identification technique.

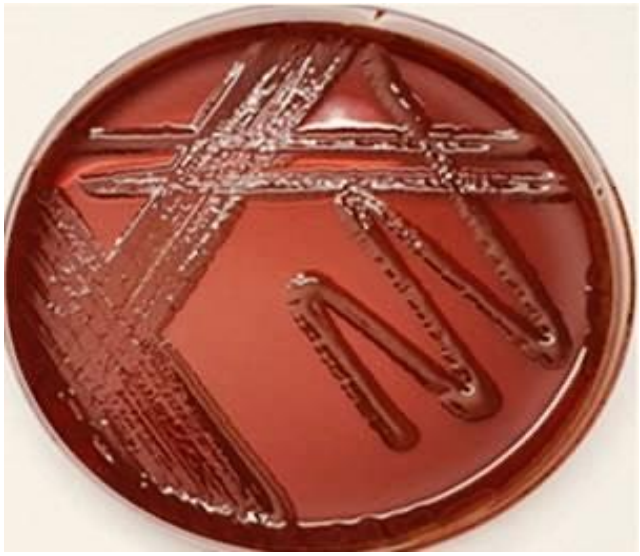

Fig. 1. A. baumannii isolates on MacConkey agar

3.2. Antibiotic susceptibility test

According to the latest investigation, clinical isolates of A. baumannii displayed substantial resistance to the majority of the antibiotics used to evaluate. In particular, isolates of A. baumannii illustrated 100% resistance to the following kinds of antibiotics: Gentamicin (CN), Tetracycline (TTC), Piperacillin, Tazobactam (TPZ), Ampicillin-Sulbactam (AMS), Ceftriaxone (CRO), Cefotaxime (CTX), Cefepime (FEP), Ceftazidime (CAZ) and Piperacillin (PRL), the following percentages among

patients showed resistance: 96.7% for Amikacin (AK), 76.7% overall for Imipenem (IMP) and Meropenem (MEM), and 66.7% for levofloxacin (LEV) as shown in Fig. 2.

3.3. Synthesis of Ch-ZnO NPs

The prepared Chitosan/ZnO nanoparticles at 120°C in powder form were then characterized, and the formation of nanoparticles was indicated by the formation of a white precipitate. After centrifugation, the precipitate appeared white. After drying with the microwave, we obtained a shiny white powder. The present study investigates the impact of Zn and CS combinations on the antibacterial activity of coated textile surfaces. To the best of our knowledge, this is the first study describing a one-step magnetic starrier approach for forming organometallic nanocomposites on fabrics.

3.4. Characterization of Ch-ZnO NPs

3.4.1 UV–Vis Spectral analysis and zeta potential analysis

The production of Ch-ZnO NPs has been established by UV-visible spectroscopic investigation. The sample was submerged in deionized water for this typical assay. As seen in Fig. 3, the results verified the production of newly produced Ch-ZnO NPs at their greatest peak at 235 nm, indicating nanoparticles in excitation form from the ground state to the excited state. Because the tiny particles in Ch-ZnO NPs are in the nasoscope, they exhibit a limited size distribution, which is evident in the strong absorption peak. As nanoparticles have significant absorption in the UV range of 200–400 nm, they are appropriate for use in medical applications such as antibacterial ointments and sunscreen defenders. The mean particle size and zeta potential of the Ch-ZnO nanoparticle were measured using a Zetasizer instrument. On the other hand, the results by Türemen et al. [21] show the UV-Vis spectra of chitosan, ZnO nanoparticles (ZnO NPs), and chitosan-zinc oxide nanocomposites (Ch-ZnO NPs) at various concentrations. To determine the optimal chitosan concentration, 0.5 g of ZnO NPs was consistently used. The spectra of the chitosan-coated samples displayed a blue shift, while the absorption peaks of the zinc nanoparticles appeared at 370 nm.

Fig. 2. Antibiotic susceptibility of Acinetobacter baumannii

3.4.2 Atomic force microscopy (AFM) analysis

AFM analysis of Ch-ZnO NPs was performed with CSPM to identify and characterize distributions of nanoparticles. The chitosan-zinc oxide (ZnO) nanocomposite's microstructure was investigated utilizing atomic force microscopy (AFM). ZnO nanoparticles were discovered to have irregular and triangle cluster morphologies, ranging between 0.25 and 34.33 nm in height and 13 to 177 nm in diameter (as verified by a particle size analyzer) according to the three-dimensional AFM as shown in Fig. 4, agreeing with Mahdi et al. [22].

AFM analysis was conducted to examine the physical properties of Ch-ZnO NPs in their dry state, revealing that the zinc nanoparticles had an approximate size of 30 nm. Furthermore, the significant changes in the size of ZnO in its hydrated state at pH 5, compared to its dry state, support its aggregation tendency. These findings are consistent with previous studies on zeta potential and hydrodynamic diameter.

3.4.3. Field emission scanning electron microscope (FESEM)

Utilizing scanning electron microscopy (SEM), the membrane's structural features and crystallinity were examined. To comprehend the size, shape, and elemental and structural composition of the NPs samples, analysis was done. Ch-ZnO NPs' spherical shape is depicted in Fig. 5 at a magnification of 13000x and 50000x. The

chitosan nanoparticles used in the experiment took on the appearance of white powder. Scanning electron micrographs of the Nanomagnetic chitosan revealed that they were about spherical. The groups of particles that make up the unaltered chitosan nanoparticles range in size from 10 to 33 nm. Images from a scanning electron microscope of chitin nanofibers made from Alaskan pink shrimp and Japanese tiger prawns, two important dietary sources. The same procedure, which includes eliminating matrix components followed by grinding the product at a neutral pH, was used for producing these chitin nanofibers [23].

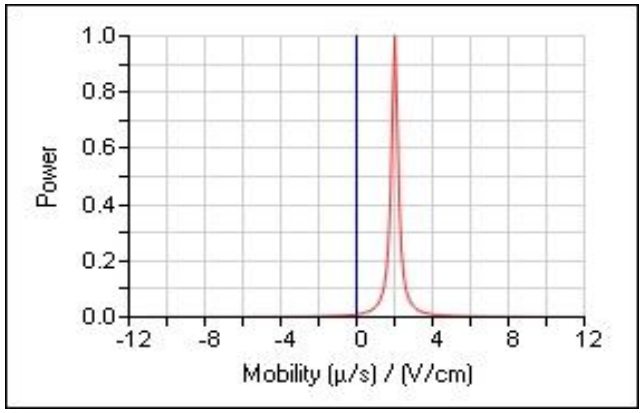

a) Mobility

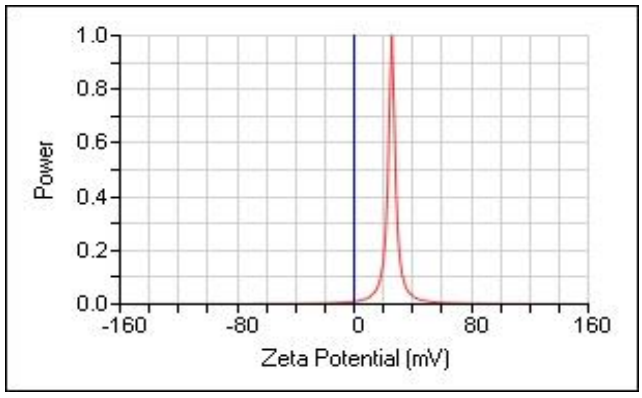

b) Zeta potential

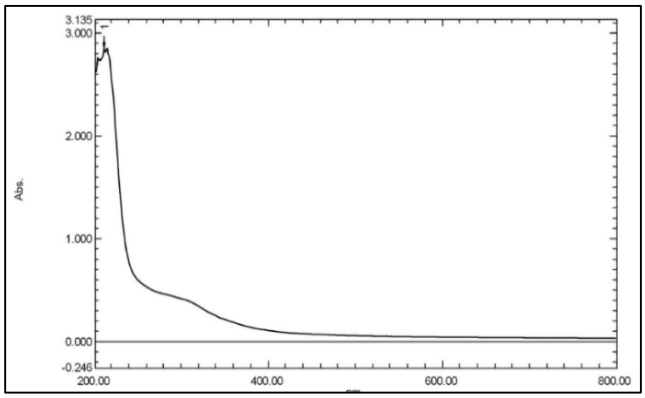

c) UV analysis

Fig. 3. a) Mobility, b) Zeta potential, and c) UV analysis of bio-synthesized Ch-ZnO NPs

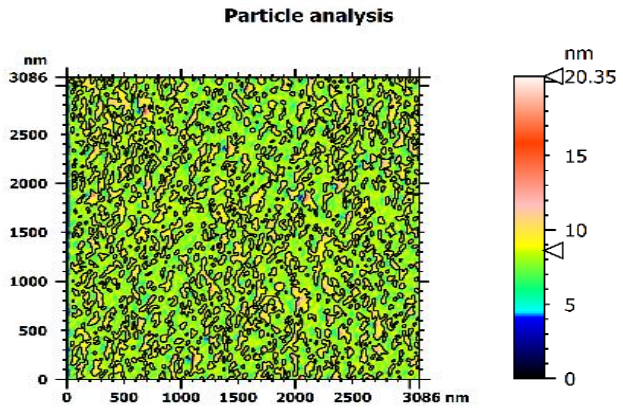

Fig. 4. Atomic force microscopy analysis of Ch-ZnO NPs

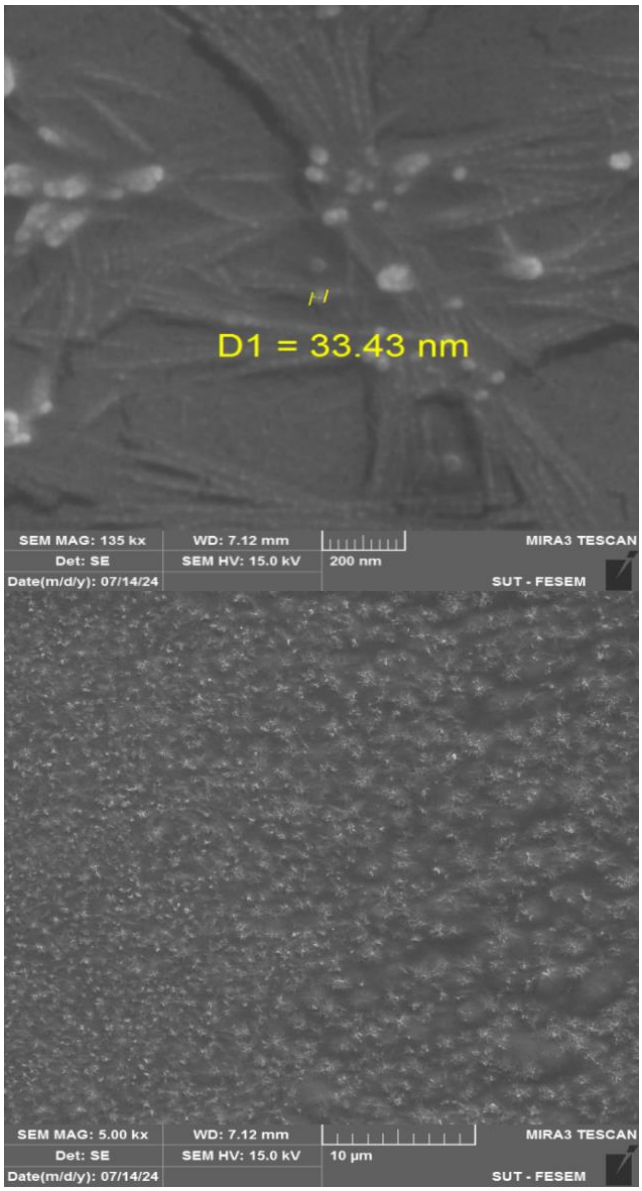

Fig. 5. FESEM images of Ch-ZnO NPs

3.4.4. X-ray diffraction XRD

The XRD patterns showed that ZnO is crystalline and that ZnO-chitosan nanotechnology had low intensities of their peaks as shown in Fig. 6, which indicates their crystallinity has decreased. With a hexagonal quartzite structure. Because the sample pattern and the standard are nearly identical, it can be said that the quartzite of Ch-ZnO NPs is hexagonal and has nine major peaks situated at (100), (002), (101), (102), (110), (103), (200), (112), and (201). The purpose of this research is to investigate the impact of chitosan modification on ZnO nanoparticles via the synthesis of ZnO/Chitosan using different molar ratios of Zn and Ch. The result by Ahmed and Abdul Muhsin [24] shows rectangular quartzite structure of ZnO nanoparticles validated the XRD pattern. The Scherrer formula was utilized to calculate the particle size; an average particle size of 25 nm was found. The ZnO-chitosan nanocomposite (ZC-NC) XRD pattern exhibited the same hexagonal quartzite structure, with each material's main peaks evident. The effective production of Ch-ZnO NPs was demonstrated by the diffraction peaks that formed, which match ZnO and chitosan. ZnO's crystal structure remained intact even after it bonded with chitosan. The morphology and elemental material of the nanoparticles have been determined using EDX methods. Images from EDX and SEM were generated. Additional EDX results were by XRD results, as ZnO and ZnO-Chitosan nanomaterials were determined to be 100% pure and only included zinc and oxygen elements [25].

3.4.5. Energy dispersive X-ray (EDX)

Ch-ZnO NPs have been identified within the polymer matrix of the Ch-ZnO nanocomposite film, as shown by energy dispersive X-ray (EDX) examination in Fig. 7, On the cylindrical particles on the coating, a single area was used to conduct the EDX profile. The spectra's Zn peaks indicate that the Ch-ZnO NPs were effectively integrated into the polymer matrix. In addition, the ZnO was found while performing the nanocomposite's elemental assessment. The minute particle size of Ch-ZnO NPs can be utilized to clarify their antimicrobial action since smaller materials can penetrate the membranes of bacteria and destroy cells. Multiple studies have previously shown the anti-biofilm activity of NPs; one study showed a concentration-dependent, significant decrease in the creation of biofilm of different species of microorganisms after treatment with nanocomposite [26].

3.4.6. FTIR analysis

The carbonyl group (-C=O) of chitosan and the C-H group of gelatins interact, as demonstrated by the hybrid composite films' FTIR spectra. Strong absorption can be detected at 3293 cm−1 (-OH stretching), 2925 cm−1 (N-H stretching of amide A), 1549 cm−1 (C-C, C stretching), 1410 cm−1 (C-O stretching), and 1640 cm−1 (C=O straining) in the FTIR spectra of the unaltered (CH/GL) specimen film as shown in Fig. 8.

3.5. Determination of biofilm formation before Ch-ZnO NPs treatment

A total of 10 MDR isolates were tested for their biofilm production ability using a plastic flat-bottom microtiter plate. In Fig. 9, eight isolates were recorded as strong biofilm producers: Y2, Y5, Y1, Y4 Y3, Y8, Y10 and Y6 (20%, 19%, 19%, 14%, 10%, 8%, 6% and 6%), respectively, as detailed in Fig. 10. To estimate the effect of Ch-ZnO NPs Eight strains of strong producers have been selected based on the biofilm production of these isolates. With the aid of a microtiter plate reader, the OD of every well was obtained at 630 nm. The biofilm formation of used isolates from patients can be seen in Fig. 9. Several antimicrobial agents and antibiofilm, comprising nanoparticles derived from different sources, such as Silver NPs produced from date palm extract for combating K. pneumonia and E. coli, consider the formation of biofilms as a target [27]. The microbe components eDNA, a component essential for bacterial adhesion, aggregation, biofilm production and integrity, intercellular communication, and QS for genetic information transfer, represent some of the many levels and targets that nanoparticles can affect [28, 29]. Because peptides have several duties they can be destroyed when they are inhibited. This can also happen to biofilm and planktonic cell membranes. Therefore, one of the primary targets of current antimicrobial therapies is proteins [30]. The substitute's antibiofilm's negative resonance effect caused their minimum inhibitory concentration (MIC) amounts to decrease. The Ch-ZnO NPs composites suggested superior inhibitory effects against all investigated Gram-positive bacteria, all tested Gram-negative bacteria, and all investigated fungi [31].

3.6. Determination of biofilm formation after Ch-ZnO NPs treatment

Biofilm production was significantly reduced after 48 hours of incubation in 37C with a sub-MIC of Ch-ZnO NPs; OD measurement of the same six strains of A. baumannii lowered from strong to weak production, as detailed in Table 1 and Fig. 11.

3.7. Cytotoxic effect of Ch-ZnO NPs

The cell line WRL 68 was originally thought to be derived from the embryonic liver. The cell line used to measure the cytotoxic effect viability was reduced to half after treatment with the nanocomposite (298.2 mg/L IC50); Fig. 12 shows cell viability getting lowered with the nanocomposite concentration increment. The cytotoxic effect of copper nanoparticles generally depends on the physicochemical properties, including particle shape, size, aggregation, crystallinity, and surface coating. A-375 is a cell line isolated from the skin of a patient with malignant melanoma cells used in this research that shows reduced viability after treatment with Ch-ZnO NPs in a dose-dependent matter. The IC50 value of nanocomposite that inhibits cell line viability is 141.5 mg/l. According to

the data collected by this test, cancer cell viability was much lower than WRL 68 cells in the same concentrations. This leads to the conclusion that Ch-ZnO NPs had a greater effect on cancer cells. To discover if nanoparticles may serve as anti-cancer agents in human and animal models, their anti-cancer activity has been extensively examined. The most frequently referenced model of cell death following exposure to metal-based nanoparticles is apoptosis; necrosis is the second model, with around half as much information. It has also been observed that a third pathway of nanoparticle cytotoxicity in cancer cells involves autophagy activation, which leads to the breakdown of enzymes and cell compartments [32]. On the other together, in the previous few years, research has focused on copper toxicity. Regarding copper toxicity, neurological disorders such as Alzheimer's disease which are categorized as copper intolerance have been associated with copper toxicity. Histopathological deviations oxidative stress, and tissue inflammation may additionally arise from nanoparticle relationships [33]. Showing that the interaction between LPS and NPs was mostly affected by electrostatic interactions. This behavior can be explained by the reactive oxygen species that develop when oxidative stress is applied by nanoparticles, thereby destroying the mitochondria of bacteria. Also, studies revealed that applying nanoparticles to bacteria caused a significant decrease in their membrane potential, showing that the materials may target their cell membranes.

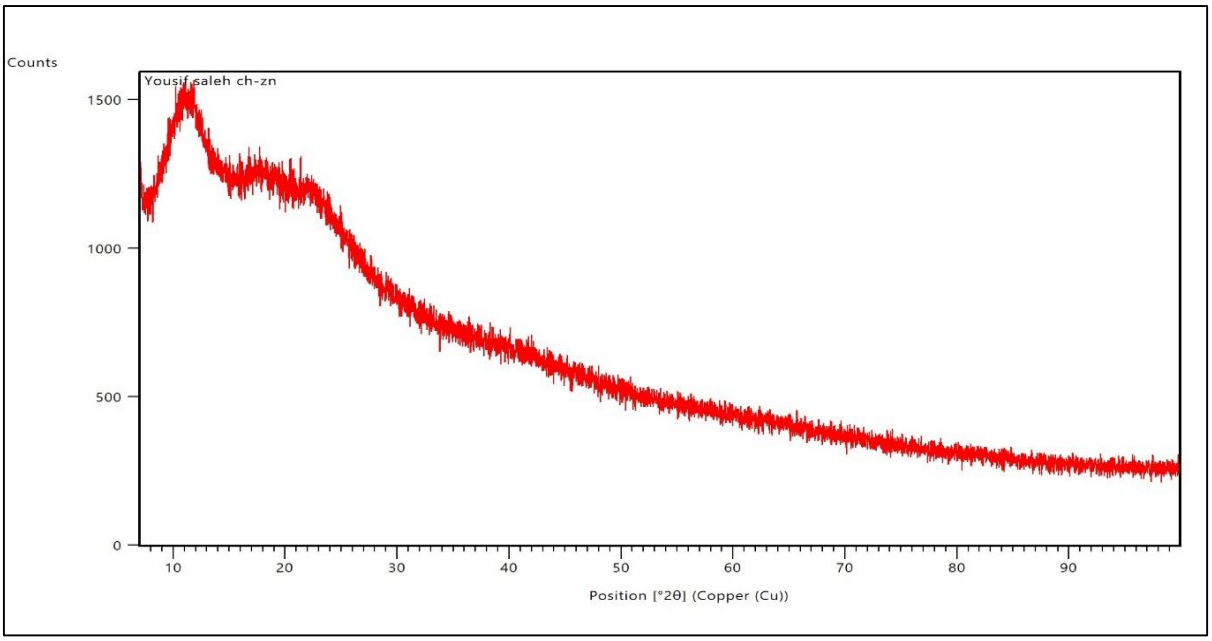

Fig. 6. XRD analysis of synergistic Ch-ZnO NPs

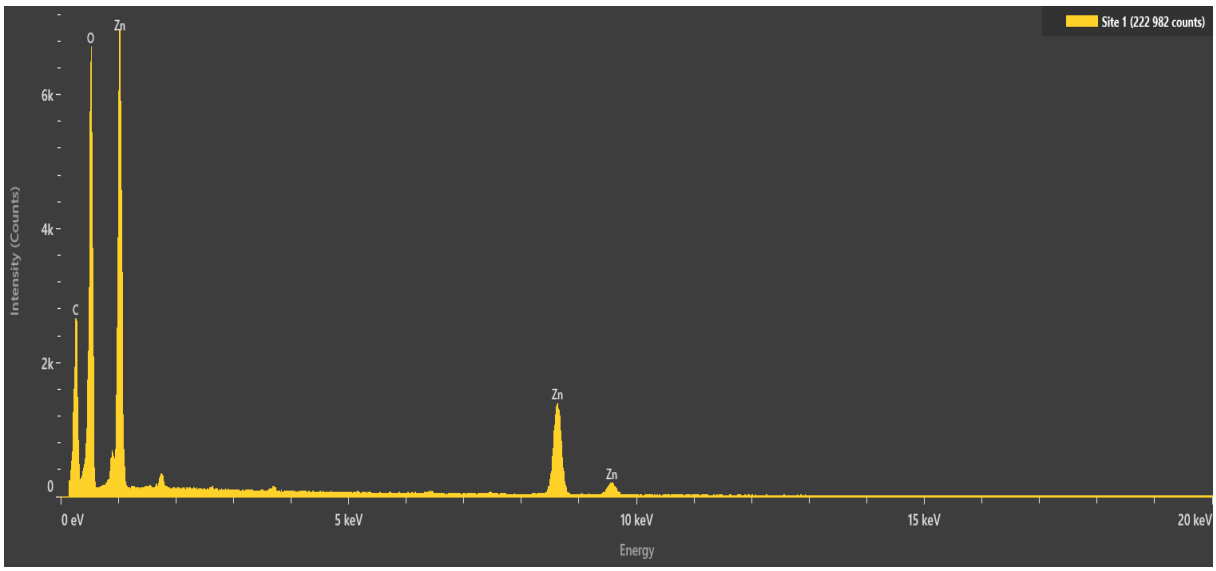

Fig. 7. EDX of Ch-ZnO NPs

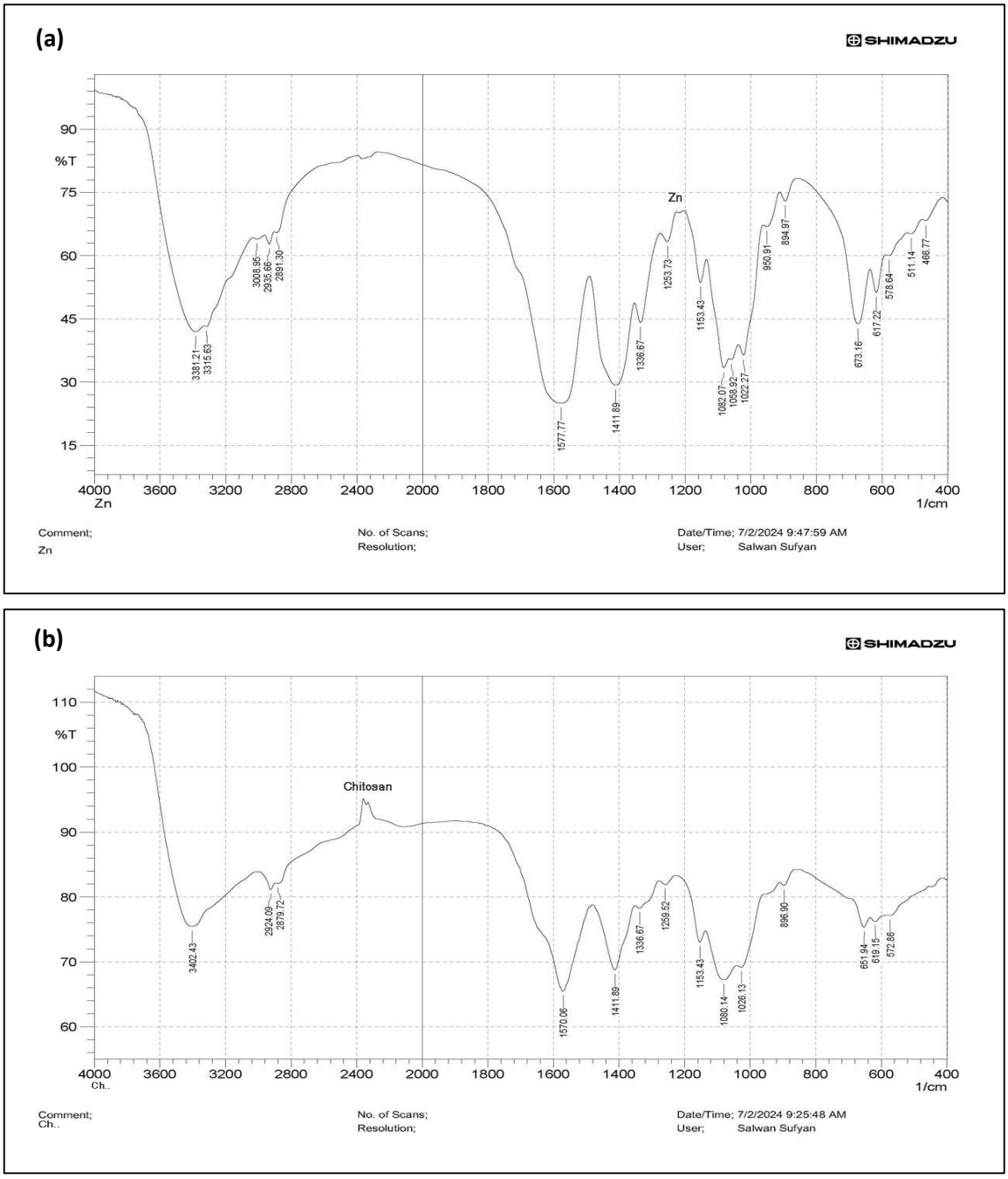

Fig. 8. Fourier-transform infrared spectroscopy (FTIR) a) Zn & b) Chitosan

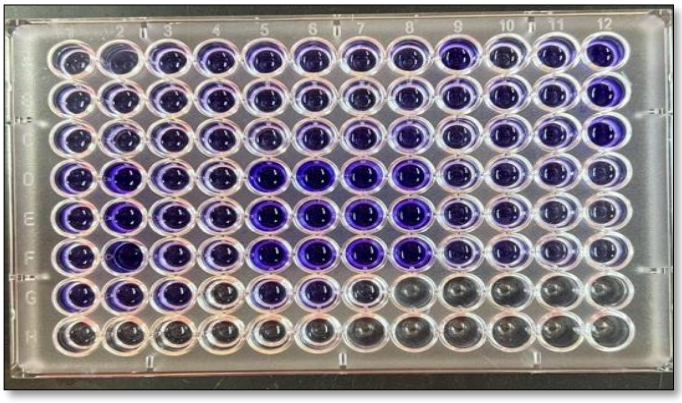

Fig. 9. Microtiter plate assay for biofilm production

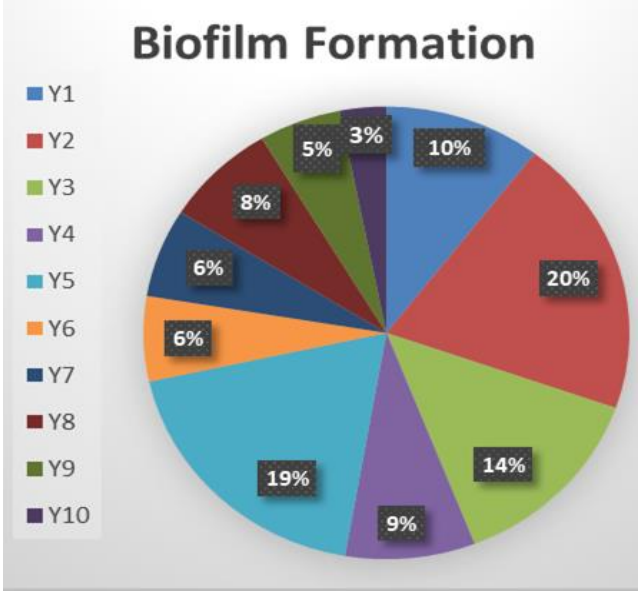

Fig. 10. Percentage of biofilm values of A.baumannii

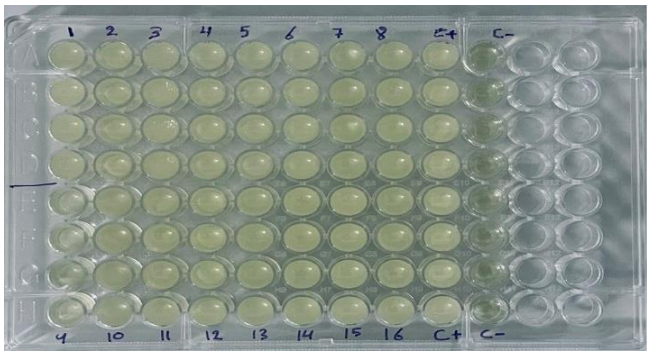

Fig. 11. Biofilm production after treatment with Ch-ZnO NPs

Table 1. O.D values before and after treatment with Ch-ZnO NPs

NO. of isolate	O.D Before treatment	O.D after treatment with CS/ZnONPs
Y1	5.75	1.0
Y2	9.19	1.45
Y3	6.30	1.11
Y4	7.25	1.14
Y5	7.55	1.17
Y6	7.23	1.16
Y8	6.12	1.26
Y10	6.0	1.44

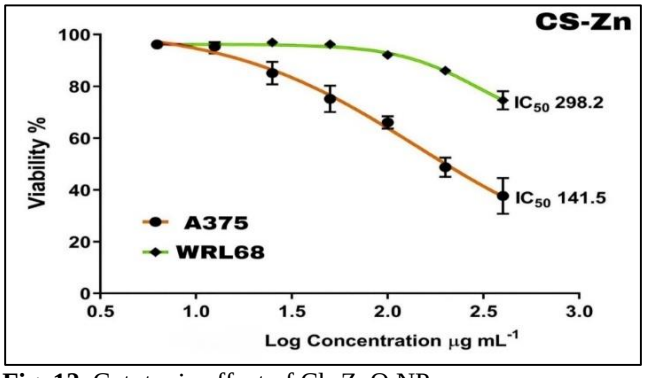

Fig. 12. Cytotoxic effect of Ch-ZnO NPs

4-

5- Conclusion

This study is designed to formulate and characterize experiments containing CH-ZnO nanoparticles (CH-ZnO NPs) and investigate their antimicrobial effects on both planktonic and biofilm forms of A. baumannii. The microbial load was reduced because of the synergistic effect between chitosan and ZnO nanoparticles. This work aims to develop a type of bio nanocoating that multidrug-resistant bacteria may utilize in their reduced biofilm. It contains biological biopolymer chitosan and inorganic nanostructured materials ZnO. These metal oxides have some limitations when utilized in manufactured nanocomposites, primarily used in medication delivery and medical procedures due to their increased toxicity at higher concentrations. The preceding results all suggest the necessity of more research to employ CH-ZnO NPs as potentially beneficial alternative antibacterial materials and in anti-cancer applications.

References

[1] S. Roy, G. Chowdhury, A. K. Mukhopadhyay, S. Dutta, and S. Basu, "Convergence of biofilm formation and antibiotic resistance in *Acinetobacter baumannii* infection," *Frontiers in Medicine*, vol. 9, 2022, Art. no. 793615. https://doi.org/10.3389/fmed.2022.793615

[2] M. F. Salman and A. M. N. A. ME, "The effect of selenium nanoparticles on the expression of MexB gene of *Pseudomonas aeruginosa* isolated from wound and burn infections," *Iraqi Journal of Medical Sciences*, vol. 22, no. 1, pp. 79–92, 2024.

[3] M. E. Ahmed and S. H. Seddiq, "Effects of bacteriocin from MRSA and *Pseudomonas aeruginosa* against biofilm of foodborne pathogen," *Plant Archives*, vol. 18, no. 2, pp. 2770–2776, 2018.

[4] A. Chukamnerd *et al.*, "Association of biofilm formation, antimicrobial resistance, clinical characteristics, and clinical outcomes among *Acinetobacter baumannii* isolates from patients with ventilator-associated pneumonia," *The Clinical Respiratory Journal*, vol. 18, no. 1, pp. e13732, 2024. https://doi.org/10.1111/crj.13732

[5] H. H. Muunim, M. T. Al-Mossawei, and M. E. Ahmed, "Comparative study among the MRSAcin, Nisin A, and vancomycin on biofilm formation by methicillin-resistant *Staphylococcus aureus* isolated from food sources," *International Journal of Drug Delivery Technology*, vol. 39, no. 3, pp. 176–181, 2019.

[6] M. Emad and K. Salama, "Comparison of the effects of lemon peel-silver nanoparticles versus brand toothpastes and mouthwashes on *Staphylococcus spp.* Isolated from dental caries," *Iraqi Journal of Science*, vol. 61, no. 8, pp. 1894–1901, 2020. https://doi.org/10.24996/ijs.2020.61.8.6

[7] S. H. Seddiq, A. M. Zyara, and M. E. Ahmed, "Evaluation of the antimicrobial action of kiwifruit zinc oxide nanoparticles against *Staphylococcus aureus* isolated from cosmetics tools," *BioNanoScience*, pp. 1–10, 2023. https://doi.org/10.1007/s12668-023-01142-1

[8] S. M. Mahdi, M. E. Ahmed, and A. F. Abbas, "Effect of enterocin–zinc oxide nanoparticles on gene expression of rsbA swarming genes in *Proteus mirabilis* isolated from catheter urine," *Biomedical and Pharmacology Journal*, vol. 17, no. 2, 2024. https://dx.doi.org/10.13005/bpj/2939

[9] N. Jaber *et al.*, "Review of the antiviral activity of chitosan, including patented applications and its potential use against COVID-19," *Journal of Applied Microbiology.*, vol. 132, pp. 41–58, 2022. https://doi.org/10.1111/jam.15202

[10] J. Li and S. Zhuang, "Antibacterial activity of chitosan and its derivatives and their interaction mechanism with bacteria: current state and perspectives," *European Polymer Journal*, vol. 138, Art. no. 109984, 2020. https://doi.org/10.1016/j.eurpolymj.2020.109984

[11] M. Abbasi *et al.*, "Inhibitory effect of zinc oxide nanoparticles and fibrillar chitosan-zinc oxide nanostructures against herpes simplex virus infection," *The Journal of Engineering*, vol. 2023, no. 6, Art. no. e12268, 2023. https://doi.org/10.1049/tje2.12268

[12] M. E. Ahmed, M. Q. Al-lam, and D. D. M. Abd Ali, "Evaluation of the antimicrobial activity of plant extracts against bacterial pathogens isolated from urinary tract infections among male patients," *Al-Anbar Medical Journal*, vol. 17, no. 1, pp. 20–24, 2021. https://doi.org/10.33091/amj.2021.171060

[13] A. E. Rashid, M. E. Ahmed, and M. K. Hamid, "A Green synthesized zinc oxide nanoparticles against MRSA wound healing in vivo," *Journal of Nanostructures*, 2023. https://doi.org/10.22052/JNS.2023.04.008

[14] Z. J. S. Hassan, M. K. Hamid, and M. E. Ahmed, "Synthesized zinc oxide nanoparticles by the precipitation method on *Streptococcus spp.* from dental caries and cytotoxicity assay," *International Journal of Drug Delivery Technology*, vol. 12, pp. 1327–1330, 2022. https://doi.org/10.25258/ijddt.12.3.65

[15] E. A. Dil *et al.*, "Biocompatible chitosan-zinc oxide nanocomposite based dispersive micro-solid phase extraction coupled with HPLC-UV for the determination of rosmarinic acid in the extracts of medicinal plants and water samples," *The International Journal of Biological Macromolecules*, vol. 154, pp. 528–537, 2020. https://doi.org/10.1016/j.ijbiomac.2020.03.132

[16] Z. M. Romi and M. E. Ahmed, "Influence of biologically synthesized copper nanoparticles on biofilm formation by *Staphylococcus haemolyticus* isolated from seminal fluid," *Iraqi Journal of Science*, vol. 1948–1968, 2024. https://doi.org/10.24996/ijs.2024.65.4.15

[17] A. E. Rashid, M. E. Ahmed, and M. K. Hamid, "Evaluation of antibacterial and cytotoxicity properties of zinc oxide nanoparticles synthesized by the precipitation method against methicillin-resistant *Staphylococcus aureus*," *International Journal of Drug Delivery Technology.*, vol. 12, no. 3, pp. 985–989, 2022. https://doi.org/10.25258/ijddt.12.3.11

[18] R. P. Patel, H. H. Patel and A. H. Baria, "Formulation and Evaluation of Carbopol Gel Containing Liposomes of Ketoconazole. (Part-II)," *International Journal of Drug Delivery Technology*, vol. 1, no. 2, pp. 42–45, 2009.

[19] N. H. Faiq and M. E. Ahmed, "Effect of biosynthesized zinc oxide nanoparticles on phenotypic and genotypic biofilm formation of *Proteus mirabilis*," *Baghdad Science Journal*, vol. 21, no. 3, Art. no. 0894, 2024. https://doi.org/10.21123/bsj.2023.8067

[20] Z. M. Romi and M. E. Ahmed, "Synergistic effect of biosynthesized copper oxide nanoparticles and vancomycin on biofilm formation of *Staphylococcus haemolyticus*," *Ibn Al-Haitham Journal for Pure and Applied Sciences*, vol. 37, no. 2, pp. 28–40, 2024. https://doi.org/10.30526/37.2.3374

[21] M. Türemen, A. Demir, and Y. Gokce, "Synthesis and application of chitosan-coated ZnO nanorods for multifunctional cotton fabrics," *Materials Chemistry and Physics*, vol. 268, Art. no. 124736, 2021. https://doi.org/10.1016/j.matchemphys.2021.124736

[22] S. M. Mahdi, M. E. Ahmed, and A. F. Abbas, "Effect of enterocin–zinc oxide nanoparticles on gene expression of rsbA swarming genes in *Proteus mirabilis* isolated from catheter urine," *Biomedical and Pharmacology Journal*, vol. 17, no. 2, 2024. https://dx.doi.org/10.13005/bpj/2939

[23] N. S. Yousef, F. Shokry, and M. Elkhatib, "Chitosan/PVA nanofibers and membranes: Preparation, characterization, and potential applications," *Port Said Engineering Research Journal*, vol. 28, no. 1, pp. 103–111, 2024. https://doi.org/10.21608/pserj.2023.228866.1255

[24] M. E. Ahmed and Z. A. Abdul Muhsin, "Synergistic effect of gentamicin and iron oxide nanoparticles on *phzM* gene of *Pseudomonas aeruginosa*," *Journal of Microbiology*, vol. 86, no. 3, pp. 27–39, 2024. https://doi.org/10.15407/microbiolj86.03.027

[25] N. H. H. Faiq and M. E. Ahmed, "Inhibitory effects of biosynthesized copper nanoparticles on biofilm formation of *Proteus mirabilis*," *Iraqi Journal of Science*, pp. 65–78, 2024. https://doi.org/10.24996/ijs.2024.64.1.7

[26] M. E. Ahmed, A. Q. Al-Awadi, and A. F. Abbas, "Focus on synergistic bacteriocin-nanoparticles enhancing antimicrobial activity assay," *Journal of Microbiology*, vol. 85, no. 6, pp. 95–104, 2023. https://doi.org/10.15407/microbiolj85.06.095

[27] L. S. Mohammed and M. E. Ahmed, "Effects of ZnO NPs on *Streptococcus pyogenes* in vivo," *Ann Trop Med Public Health*, vol. 23, no. IIb, pp. S452, 2020.

[28] M. E. Ahmed, Z. Z. Khalaf, J. A. Ghafil, and A. Q. Al-Awadi, "Effects of silver nanoparticles on biofilms of *Streptococcus spp.*," *Indian Journal of Public Health Research & Development*, vol. 9, pp. 1216, 2018. https://doi.org/10.5958/0976-5506.2018.02016.8

[29] M. E. Ahmed and A. R. Kadhim, "Effects of bacteriocin from MRSA and *Nigella Sativa* (seed oil) against biofilm from MRSA," *International Journal of Pharmaceutical Quality Assurance*, vol. 9, no. 2, pp. 199–203, 2018. https://doi.org/10.25258/ijpqa.v9i2.13647

[30] M. E. Ahmed, "Study of bacteriocin of *Pseudomonas fluorescens* and *Citrus limon* effects against *Propionibacterium acnes* and *Staphylococcus epidermidis* in acne patients," *Journal of Physics: Conference Series*, vol. 1003, no. 1, Art. no. 012004, 2018. https://doi.org/10.1088/1742-6596/1003/1/012004

[31] R. A. Alharbi *et al.*, "Design, synthesis, and characterization of novel bis-uracil chitosan hydrogels modified with zinc oxide nanoparticles for boosting their antimicrobial activity," *Polymers*, vol. 15, no. 4, Art. no. 980, 2023. https://doi.org/10.3390/polym15040980

[32] N. H. H. Faiq and M. E. Ahmed, "Synergistic inhibitory effect of biosynthesized ZnO-CuO nanocomposite on biofilm formation of *Proteus mirabilis*," *Ibn Al-Haitham Journal for Pure and Applied Sciences*, vol. 37, no. 2, pp. 51–66, 2024. https://doi.org/10.30526/37.2.3383

[33] Z. H. Kadhim, M. E. Ahmed, and I. Şimşek, "Biologically synthesized copper nanoparticles from *S. epidermidis* on resistant *S. aureus* and cytotoxic assay," *Bionatura*, vol. 8, no. 1, 2023. https://doi.org/10.21931/RB/CSS/2023.08.01.54

دراسة تأثير جسيمات الكيتوسان – الزنك النانوية (Ch-ZnO NPs) على تكوين الأغشية الحيوية الحيويه لبكتريا Acinetobacter baumannii واختبار السمية الخلوية

يوسف صالح عبد الجبار [١]، اومت غازي [١]، ميس عماد احمد [٢،*]

١ قسم علم الاحياء المجهرية الطبية وعلم الاحياء الامجهرية السريرية، كلية الطب، جامعة الشرق الادنى، نيقوسيا، قبرص
٢ قسم علوم الحياة، كلية العلوم، جامعة بغداد، بغداد، العراق

الخلاصة

كان هدف البحث هو إنشاء واختبار جسيمات نانوية من أكسيد الزنك الكتوسان (Ch–ZnO NPs) ، لاستخدامها كعوامل لمكافحة الأغشية الحيوية التي تنتجها بكتيريا Acinetobacter baumannii متعددة الأدوية، واستكشاف استخداماتها الطبية. تم إنتاج جسيمات نانوية من أكسيد الزنك الكتوسان باستخدام الكتلة الحيوية الكتوسان كمواد صديقة للبيئة ومنخفضة التكلفة، لأغراض التوليف. تم تحليل خصائص الجسيمات النانوية الناتجة من خلال مجموعة من الأساليب. تم إجراء تحديد البنية الكيميائية وتحليلها باستخدام التحليل. مطيافية الأشعة تحت الحمراء بتحويل فوريه (FTIR). تم تأكيد ذروة الامتصاص القصوى، عند ٢٣٥ نانومتر من خلال مطيافية الأشعة فوق البنفسجية. تم التحقق من البنية البلورية السداسية بواسطة حيود الأشعة السينية (XRD) مع قياس حجم الجسيمات ٣٤ نانومتر. تمت ملاحظة مورفولوجيا السطح باستخدام المجهر الذري للقوة (AFM) والمجهر الإلكتروني الماسح للانبعاث الميداني (FESEM). تم الحصول على مزيد من التفاصيل حول بنية الجسيمات من خلال المجهر الإلكتروني النافذ عالي الدقة (HR-TEM). كان تقييم كيفية أداء جزيئات Ch–ZnO النانوية في سيناريوهات العالم الحقيقي عند التعامل مع عدوى بكتيرية Acinetobacter baumannii ومعالجة الأغشية الحيوية بشكل فعال هو محور الدراسة، مع استكشاف تأثيرها على السمية الخلوية باستخدام نموذج خط الخلية A375 للتطبيقات الطبية المحتملة. أشارت نتائج البحث إلى أن جزيئات Ch–ZnO النانوية أظهرت قدرات في تثبيط نمو الأغشية الحيوية من سلالات بكتيريا Acinetobacter baumannii المقاومة للأدوية بتركيز IC50 يبلغ ٢,٠ جم / مل، وأبرز تقييم معدلات وفيات الخلايا ارتفاعًا في وفيات الخلايا بين الخلايا المعالجة من تطبيق جزيئات Ch-ZnO النانوية. كشف البحث أن جزيئات Ch-ZnO النانوية أظهرت خصائص مضادة للأغشية الحيوية وتأثيرات سامة للخلايا مما يشير إلى إمكاناتها للاستخدام كبيرة. تؤكد هذه الدراسة على إمكانات جزيئات Ch-ZnO NPs كخيار فعال لعلاج الالتهابات المقاومة للمضادات الحيوية المتعددة.

الكلمات الدالة: الاغشية الحيوية، كيتوسان، اوكسيد الزنك، الراكدة البومانية.